

Preparation, Characterizations and Theoretical Calculations of a Mg(II) Porphyrin Complex with Axial O-bonded 4-Pyrrolidinopyridine

Souhir Jabli^a, Bouzid Gassoumi^b, Soumaya Nasri^{a,c}, H. Ghalla^b, Emiliano Martinez Vollbert^d, Florian Molton^d, Frédérique Loiseau^d, Thierry Roisnel^e, Habib Nasri^{a,}*

^a: University of Monastir, Laboratory of Physical Chemistry of Materials (LR01ES19), Faculty of Sciences of Monastir, Avenue de l'environnement, 5019 Monastir, Tunisia.

^b: Laboratory of Advanced Materials and Interfaces (LIMA), University of Monastir, Faculty of Science of Monastir, Avenue of Environment, 5000 Monastir, Tunisia

^c: Department of Chemistry, College of Science Al-Zulfi, Majmaah University, 11952, Saudi Arabia.

^d: Département de Chimie Moléculaire, 301 rue de la Chimie, Université Grenoble Alpes, CS 40700, 38058 Grenoble, Cedex 9, France

^e: Institute of Chemical Sciences of Rennes, UMR 6226, University of Rennes 1, Beaulieu Campus, 35042 Rennes, France.

Contents

| | |
|---|---|
| Section 1. ¹ H NMR spectroscopy..... | 2 |
| Section 2. IR Spectroscopy..... | 3 |
| Section 3. UV/Vis..... | 4 |
| Section 4. Crystallography..... | 4 |
| Section 5. Hirshfeld surface analysis | 5 |

Section 1. IR Spectroscopy

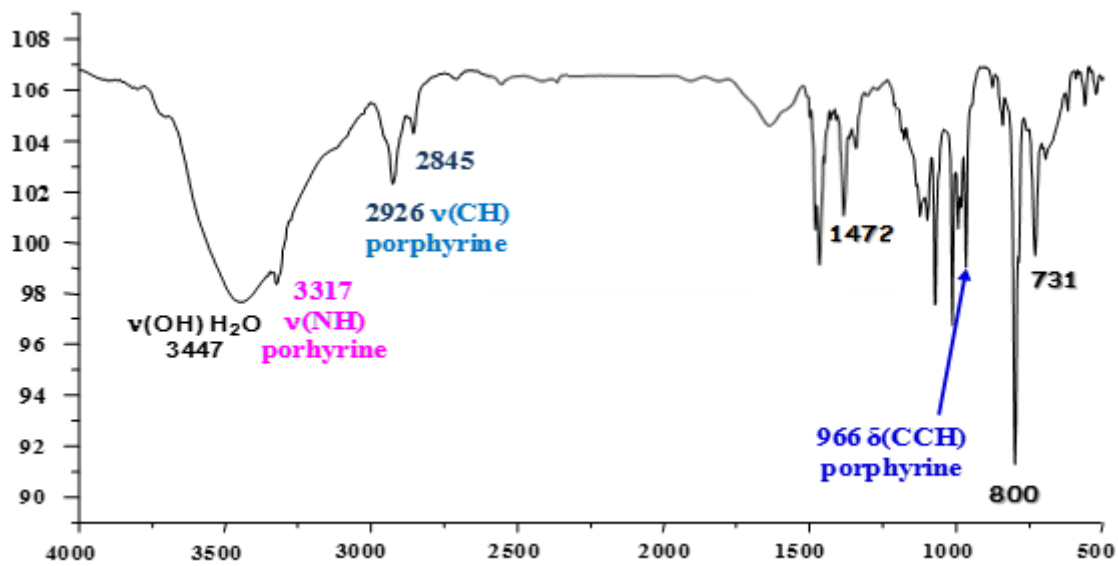


Fig. S1. IR spectrum of the H₂TBrPP free base porphyrin.

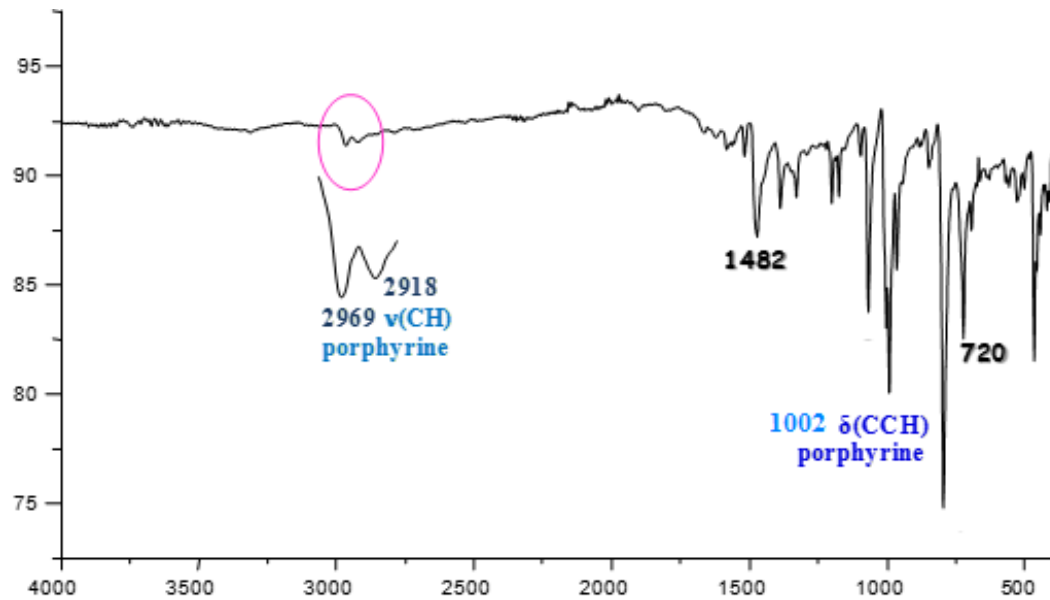
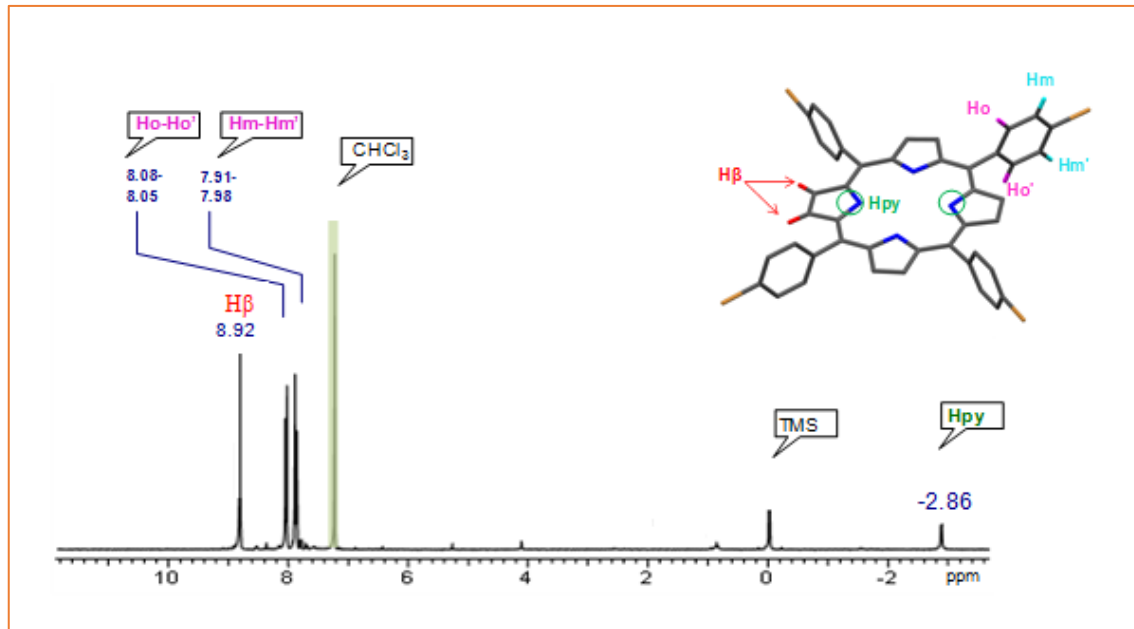


Fig. S2. Neat IR spectrum of [Mg(TBrPP)]



Section 2. ^1H NMR Spectroscopy

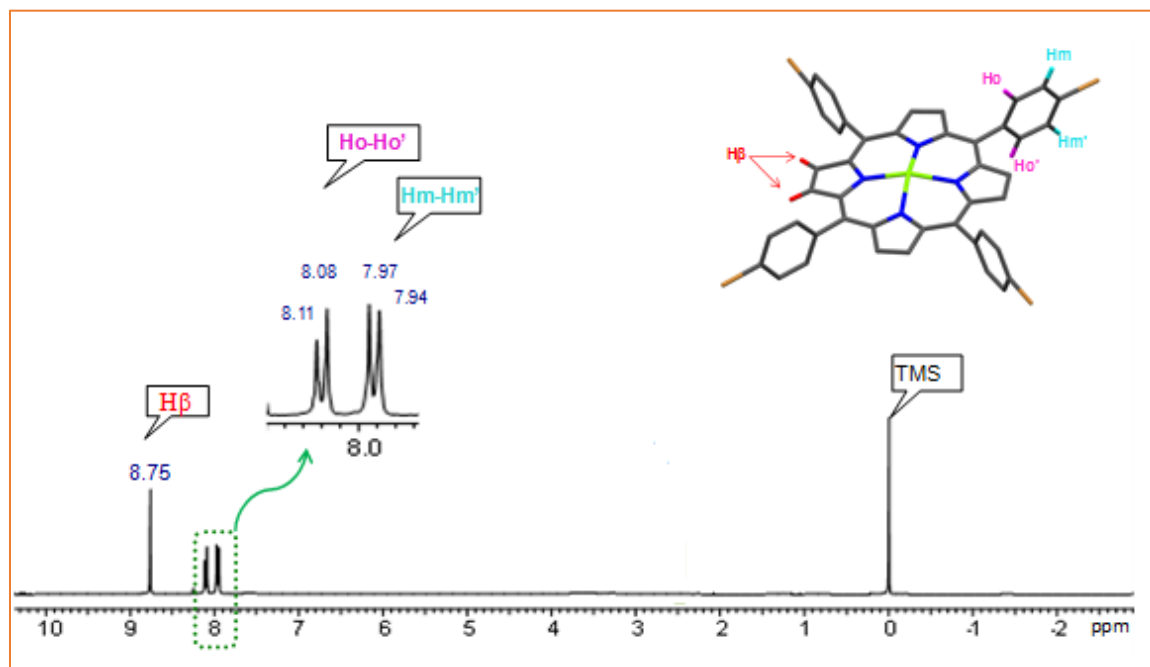


Fig. S3. ^1H NMR spectrum of the H_2TBrPP free base porphyrin recorded in CDCl_3 at room temperature with concentration $C \sim 10^{-3} \text{ M}$.

Fig. S4. ^1H NMR spectrum of the $[\text{Mg}(\text{TBrPP})]$ recorded in CDCl_3 at room temperature with concentration $C \sim 10^{-3}$ M.

Section 3: UV/Vis spectroscopy

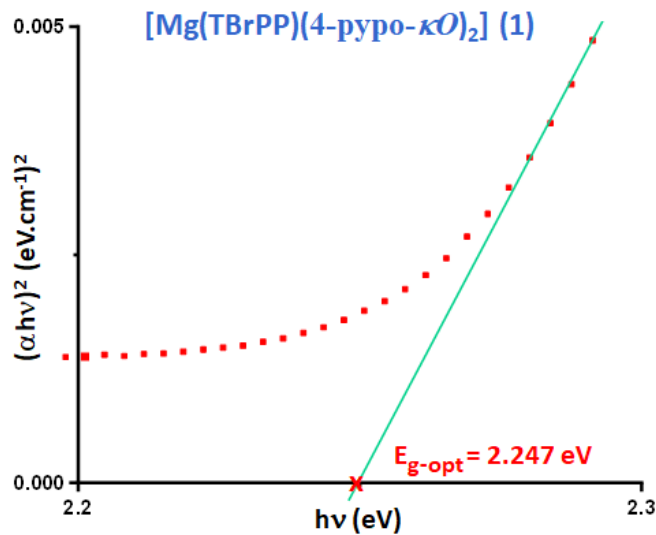


Figure S5. Plots of $(\alpha h\nu)^2$ versus the photon energy ($h\nu$) complex **1**. $h\nu$ is the incident photon energy and α is the absorption coefficient.

Section 4: Crystallography

Table S1. π - π interactions (\AA , $^\circ$) in the crystal structure of complex **1**.

| $Cg(I)$ | $Cg(J)$ | $Cg \dots Cg$ | α | CgI_{Perp} | CgJ_{Per} | <i>Slippage</i> |
|---------|---------|---------------|----------|--------------|-------------|-----------------|
| Cg3 | Cg4 | 3.998(4) | 23.1 | 25.9 | 3.598(3) | 3.873(2) |
| Cg4 | Cg3 | 3.998(4) | 23.1 | 14.4 | 3.872(2) | 3.598(3) |

$Cg...Cg$ = distance between ring centroids, α = dihedral planes I and J , CgI_Per = perpendicular distance of CgI on ring J , CgJ_Perp = perpendicular distance of CgI on ring I .

$Cg3$ = centroid of the five membered ring N3/C23-C24-C25-C26 of 4-pipo- κO axial ligand.

$Cg4$ = centroid of the pyridyl ring N4/C29-C28-C27-C31-C32 of a 4-pipo- κO axial ligand

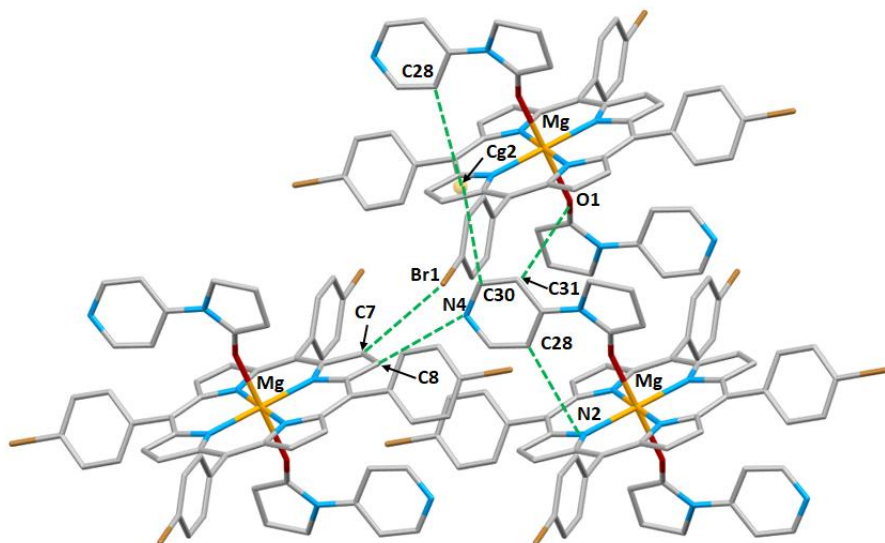


Figure S6. Drawing illustrating the C–H \cdots N, C–H \cdots O and C–H \cdots Br intermolecular interactions in complex **1**.

Table-S2. Selected intermolecular interactions for complex **1**.

| D–H \cdots A ^a | Symmetry of A | D \cdots A (Å) | D–H \cdots A (°) |
|-----------------------------|----------------|------------------|--------------------|
| C28-H28...N2 | -x,-y+2,-z+2 | 3.674(5) | 169 |
| C31-H31...O1 | -x+1,-y+2,-z+2 | 3.447(6) | 132 |
| C31-H31...N2 | -x+1,-y+2,-z+2 | 3.687(8) | 130 |
| C7-H7...Br1 | -x+1,-y+1,-z+1 | 3.752(5) | 142 |
| C8-H8...N4 | x,+y,+z-1 | 3.479(6) | 151 |
| C28-H28...Cg2 | -x,2-y,2-z | 3.568(8) | 151 |
| C30-H30...Cg2 | 1-x,2-y,2-z | 3.574(8) | 140 |

^a: D = donor atom and A = acceptor atom.

Cg2: is the centroid of the pyrrole ring N2/C6-C9

Section 5: Hirshfeld surface analysis

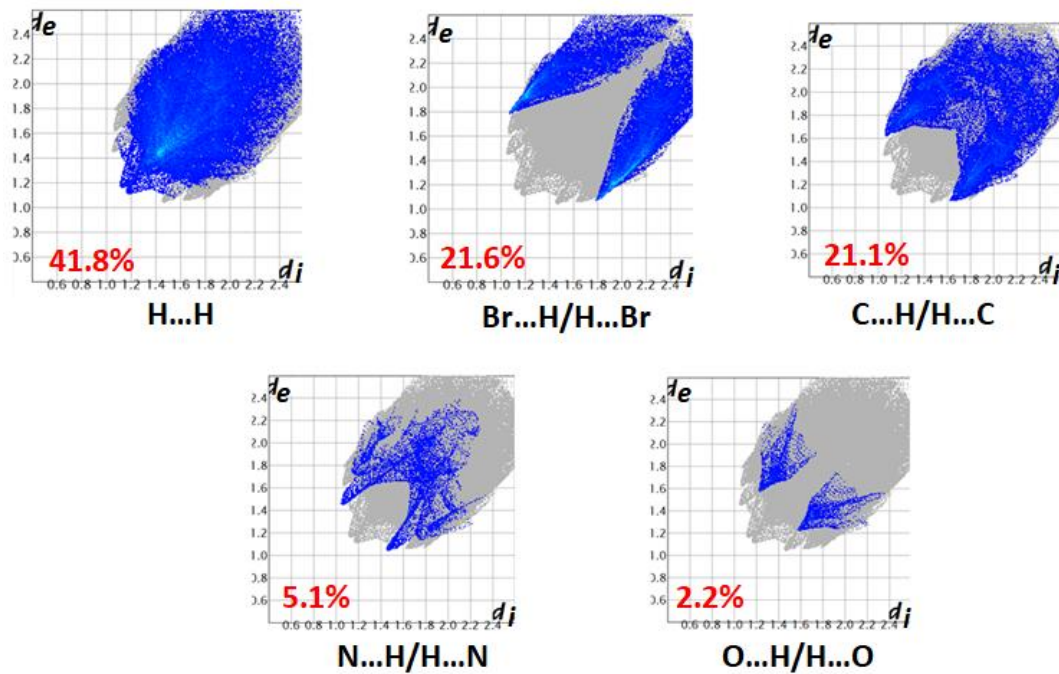


Figure S7. Decomposed fingerprint plots for the dominant interactions in complex **1**.